Journal of Visualization, Vol. 9, No. 1 (2006)23-30

PIV Studies of Large Scale Structures in the Near Field of Small Aspect Ratio Elliptic Jets

Ramesh, G.*[1], Venkatakrishnan, L.*[1] and Prabhu, A.*[2]

*1 Experimental Aerodynamics Division, National Aerospace Laboratories, Bangalore, India.
*2 Indian Institute of Science, Bangalore, India.

Received 17 December 2004
Revised 12 July 2005

Abstract : The near flow field of small aspect ratio elliptic turbulent free jets (issuing from nozzle and orifice) was experimentally studied using a 2D PIV. Two point velocity correlations in these jets revealed the extent and orientation of the large scale structures in the major and minor planes. The spatial filtering of the instantaneous velocity field using Gaussian convolution kernel shows that while a single large vortex ring circumscribing the jet seems to be present at the exit of nozzle, the orifice jet exhibited a number of smaller vortex ring pairs close to jet exit. The smaller length scale observed in the case of the orifice jet is representative of the smaller azimuthal vortex rings that generate axial vortex field as they are convected. This results in the axis-switching in the case of orifice jet and may have a mechanism different from the self induction process as observed in the case of contoured nozzle jet flow.

Keywords : PIV, Elliptic jet, Axis-switching, Spatial filtering, Two point correlation.

1. Introduction

Turbulent jets issuing from non-circular nozzles/orifices are useful in a number of areas of interest to engineers such as combustion, reacting flows, thrust vectoring etc. These jets provide a passive flow control that helps in the improved spread and mixing in jets. Studies on jets with non-axisymmetric nozzles show that as jet spreads, its cross section can evolve through shapes similar to that at the exit with the major and minor axis interchanging, a phenomenon known as axis switching (Krothapalli et al., 1981). This is generally related to the jet growth and mixing in non-axisymmetric jets. Ho and Gutmark (1987) in their experimental study on a 2:1 aspect ratio elliptic jet observed that the mass entrainment at the end of potential core to be about 3 to 5 times that of a circular jet of equivalent area at the same Reynolds number. Hussain and Husain (1989), from the experimental studies carried out in small aspect ratio elliptic jets, observed that the flow pattern associated in these jets involves mechanisms of vortex evolution and interaction of flow instabilities. Quinn (1989) documented the results of mean flow and turbulence characteristics of 2:1 aspect ratio elliptic orifice jet. From a comparative study of the above jet with those of Ho and Gutmark (1987) and Hussain and Husain (1989) Quinn suggests that the large difference in the axis switching location is mainly due to the difference in exit geometry between these two i.e., contoured nozzle and orifice. Zaman (1996) also observes that the development of these jets is sensitive to initial conditions determined by nozzle geometry or upstream disturbance. These studies in non-axisymmetric jets were carried out using point measurement techniques and provide no direct evidence of spatial evolution of large-scale

structures in the near field of these jets. While Davis et al. (1992) used hotwire anemometry for evaluating two point correlations in space, Erickson and Karlson (1998) used LDV measurements.

The concept of coherent structures was introduced in the early 1970's by Crow and Champange (1971). An explicit demonstration of large scale structures was made by Brown and Roshko (1974) in their experiments on plane shear layer using flow visualization as this technique could give them total field of view. These large structures were identified to be quasi-periodic large vortical structures that dominated the dynamics of flow. Their experiments highlighted the fact that whole field view is very highly useful in identifying the spatial structures that are responsible for the dynamics of the shear layer. In the recent times 2D PIV measurements have provided a new avenue to study the turbulent flow field in view of the capability to acquire large ensembles of instantaneous flow field data. The availability of whole field velocity data makes the analysis easier for comparing two points in space at the same instant of time. Renewed interest in determining the correlation function has mainly arisen from its use as inputs for coherent structures. Oakley et al. (1995) used a cinematic PIV system to obtain the two-point correlation in a turbulent free shear layer.

In the present work two-point spatial correlation on the streamwise velocity fluctuations was obtained along the streamwise direction in the shear layer in the major and minor planes for contoured nozzle jet as well as the orifice jet. The two-point spatial correlation of the velocity fluctuations provided an estimate of the extent of large scale structures present in these jets. A spatial filtering technique as suggested by Piirto et al. (2001) was applied to PIV for obtaining spanwise structures in the near field. A comparison of these azimuthal vortical structures in the nozzle jet and orifice jet has been made in the context of difference in the axis switching distances.

2. Experimental Setup

2.1 Elliptic Jet

The 2D PIV experiments were carried out in the near field of 2:1 aspect ratio elliptic jets, one issuing from a contoured nozzle and the other from an orifice plate. The schematics of the nozzle and orifice are shown in Fig. 1. The elliptic nozzle has a circular section of 203 mm diameter, smoothly contoured to an elliptic section (2a = 50.8 mm and 2b = 25.4 mm) over a length of 300 mm., where 2a and 2b are major and minor axis diameter. The orifice has the same exit geometry as that of the nozzle and has a plate thickness of 10 mm. The measurements were carried out at a nominal jet exit velocity (U_e) of 22 m/sec and the Reynolds number based on the major diameter of the jet (D_{2a}) was 72,200. The flow in the jet is seeded both internally and externally with fine droplets of fog fluid generated from a locally made nebulizer that produces seed particles in the range of 5 to 15 µm. PIV recordings were carried out up to about 16 semi major diameters in two zones each spanning a square area of 200 mm by 200 mm.

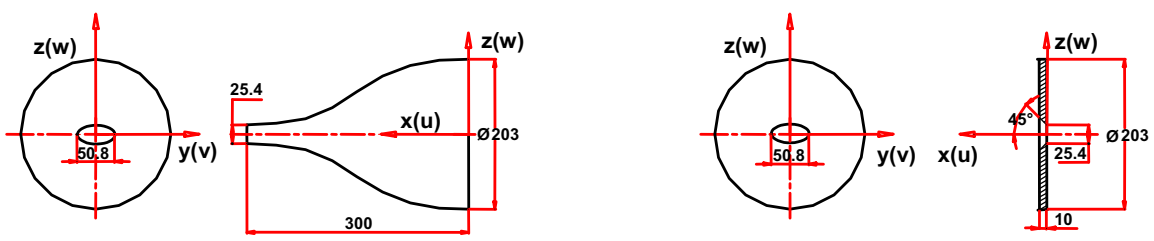

Fig. 1. Schematic of the Elliptic Nozzle and Orifice.

2.2 2D PIV System

The 2D PIV system uses a 400 mJ, dual cavity Nd: YAG laser from *Spectra Physics*, capable of pulsing at 15 pairs per second as light source. A light sheet of over 200 mm width, 1 mm thick was generated using a set of spherical and cylindrical lenses. A Kodak ES 1.0 PIV camera of 1008(H) x 1018(V) pixels with a 50 mm Nicor lens was used for recording the particle images. Synchronization of the laser pulsing with camera and also the grabbing of the images were carried out using *IDT-1000 controller* from *IDT systems* interfaced to a PC via a high speed PCI link. Image acquisition and processing were carried out using *IDT proVISION*® software that operates in Windows NT platform on a Pentium PIII PC. A pulse interval of 25 microseconds results in a particle image displacement of about 2.5 pixels for the maximum velocity in the jet. The spatial resolution of PIV was about 4.8 mm when the images were processed using 24 pixels interrogation cells. For the estimation of ensemble averaged quantities a total of 1200 frames of data from each set were used. More details of the system can be obtained from Ramesh et al. (2003).

3. PIV Studies on Nozzle and Orifice

3.1 Mean Flow Field

The mean 2D velocity vectors from the major plane of nozzle are shown in Fig. 2a. The measurements were carried out in two zones, axial distance of 200 mm each with a small overlap of 10 mm (for proper alignment) under the same exit condition. These zones are represented by two colors of the vectors. A total of 3575 averaged velocity vectors are obtained in each zone (frame) of PIV record. For clarity vectors are shown at a few axial locations only. A similar plot of the velocity vectors for the orifice jet is shown in Fig. 2b. The variation of the jet half width in nozzle and orifice both in the minor and major planes is shown in Fig. 3. The half velocity widths B_y and B_z are normalized distances (with respect to semi major diameter) from the jet centerline to the point where the mean velocity in each plane is equal to half of the centerline velocity ($U/U_c = 0.5$). In the major plane of nozzle, the jet width remained nearly constant up to 16 semi major diameters while in the orifice there is a negative growth. This can also be observed from the vector plots in Fig. 2a and Fig. 2b.

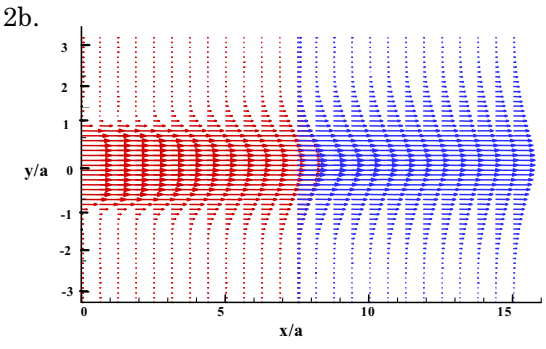

Fig. 2a. Mean Velocity Vectors in the Major Plane of Nozzle Jet.

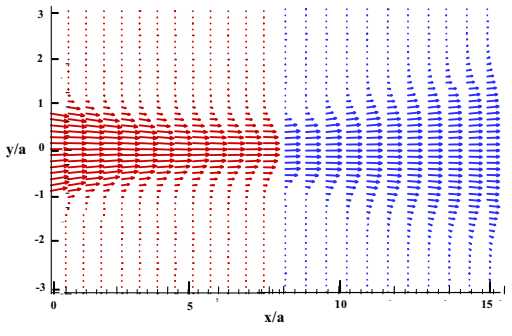

Fig. 2b. Mean Velocity Vectors in the Major Plane of Orifice Jet.

It can be seen from the Fig. 3 that in the minor plane, both nozzle jet and orifice jet showed a positive growth however the rate of growth is higher in orifice jet. We have also observed from the centerline velocity, U_c distribution (not shown here) that the orifice jet has a shorter potential core and higher decay rate compared to the nozzle jet. The higher spread in the orifice jet is consistent with its faster decay of U_c if the momentum of the jet is to be conserved. Such difference in spread rate has been observed by Sang Lee and Beak (1994) with 3D LDV measurements. They attributed the asymmetric azimuthal deformation of the vortical structures in the elliptic jet, being the reason for higher spreading in the minor plane than in major plane. The axis-switch location X_c (cross over point) is found to be at $x/a = 6.5$ in the case of nozzle jet and $x/a = 2.8$ in the case of orifice jet.

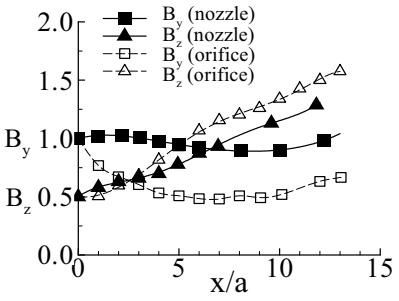

Fig. 3. Variation of the Jet Half Widths in the Major and Minor Planes.

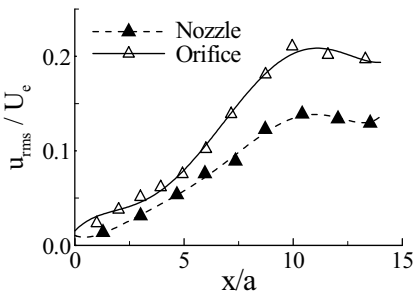

Fig. 4. Variation of Streamwise Turbulence along the Jet Centerline.

A comparison of streamwise turbulence intensities along the centerline between jets from nozzle and orifice is shown in Fig. 4. The intensities are found to be higher in orifice jet compared to nozzle jet throughout with the maximum difference of over 60% occurring at x/a ~12. However the peak intensities were found to occur at nearly the same streamwise location unlike the observations made in by Quinn (1989) who observed that the early breakdown of large scale structures the in the case of orifice could have resulted in the intensity peak moving closer to the jet exit.

3.2 Two-Point Spatial Correlation

The computation of auto correlation coefficient is a very classic way to estimate the length scales in the flow (Hinze, 1975). The auto correlation of velocity component u is defined as follows.

$$R_{uu}(\tau) = \frac{1}{T}\int_0^T u(t)u(t-\tau)dt \tag{1}$$

where τ is the lag time.

In the case of spatial correlation the time interval is replaced by space interval. In general the streamwise velocity perturbations are more pronounced as compared to transverse perturbations based on kinetic energy levels (Paschal, 1994). Another parameter in the estimation of the length scales is the spatial resolution of the PIV for a chosen configuration. In the present studies a square interrogation window size of 24 pixels restricts the lower bound for the spatial resolution.

The two-point spatial correlation function of the streamwise velocity fluctuations at a location x_0, y_0 is given by

$$R_{u'u'}(x_0, y_{0,}x, y) = \frac{\left\langle u'(x_{0,}y_0,t)u'(x,y,t)\right\rangle}{\left\langle u'(x_0,y_0,t)u'(x_0,y_0,t)\right\rangle} \tag{2}$$

where u' is the streamwise velocity fluctuation and x_0 and y_0 is any point of interest in the flow around which correlation is calculated. The averaging indicated by the brackets is the ensemble average over a number of frames for which correlation coefficient is required. A high value (typically above *1/e* of the peak) of correlation function $R_{u'u'}$ indicates the spatially coherent region. For any given (x_0, y_0) the function $R_{u'u'}$ was obtained as distribution over x and y by varying x and y over this entire flow field.

The correlation was computed from 150 realizations at a few stations in the shear layer in major and minor planes of both jets. The colored contour maps of the two-point spatial correlation at a streamwise location in the shear layer *($x_0/a \sim 6.5$, $z_0/a \sim -0.56$)* in the minor plane of nozzle jet are shown in Fig. 5. A characteristic length scale is calculated from the well-correlated contour map that may be considered as the average size of the large-scale velocity structure. A similar correlation contour plot in the minor plane of orifice at the same streamwise location *($x_0/a \sim 6.5$, $z_0/a \sim 0.45$)* is shown in Fig. 6. It is clearly seen that the size of the structure at these locations are different. The correlation extent relate to the largest scale of the structure present in the flow. Further the large

scale structure present in any shear layer is known to grow with the shear layer. The growth of the extent of the correlation coefficient in the nozzle jet (not shown here) is likely because of large scale structures being present. The smaller extent of the correlation coefficient with a nearly the same size suggest that the large scale coherent structures are absent in the orifice jet.

The average spatial extent of the correlation can be estimated by calculation of integral length scales in the streamwise and span wise defined as

$$l_{ux} = \int_0^\infty R_{u'x} dx \qquad \text{where} \quad R_{u'x} = R_{u'u'}(x_0, y_0, x, y_0) \tag{3}$$

$$l_{uy} = \int_0^\infty R_{u'y} dy \qquad \text{where} \quad R_{u'y} = R_{u'u'}(x_0, y_0, x_0, y) \tag{4}$$

In the present work length scales are estimated based on the distances at which the correlation values drop to *1/e* of the peak value (Oakley, 1995). A plot of the length scales, l_{ux} and l_{uy} (from correlation of *u'* along *x* and *y* directions respectively) at different streamwise locations in the shear layer of nozzle jet and orifice jet is shown in Fig. 7a and Fig. 7b respectively. The extent and variation of the correlation function in the major axis plane was observed to be nearly the same as in the case of minor axis plane.

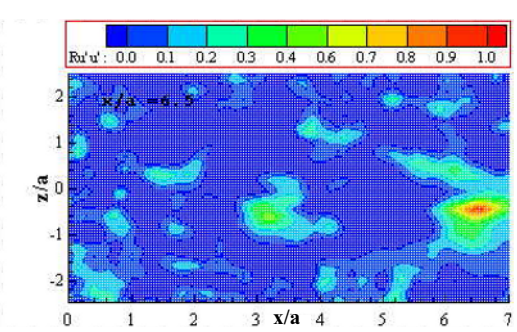

Fig. 5. Contours of Two-point Correlation in the Shear layer in Nozzle Jet.

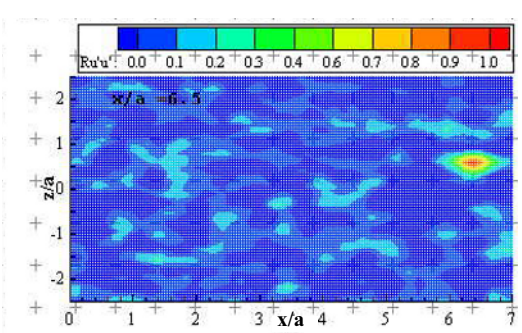

Fig. 6. Contours of the Two-point Correlation in the Shear layer in Orifice Jet.

The maximum estimated values of integral length scale l_{ux} along streamwise direction is 38 mm at x/a ~ 6.5 in the case of nozzle jet and about 20 mm in the case of orifice jet. The values of length scales (both l_{ux} and l_{uy}) are generally higher in the case of nozzle jet thus indicating presence of growing larger structures.

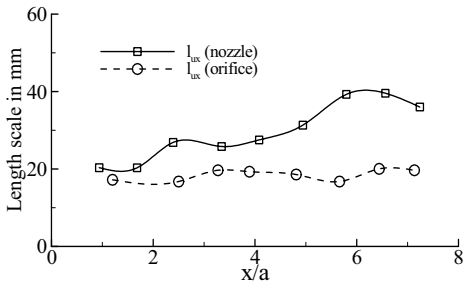

Fig. 7a. Integral Length scales in Streamwise Direction.

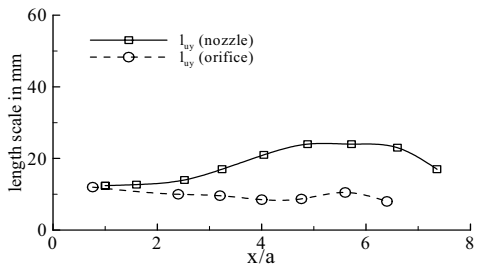

Fig. 7b. Integral Length scales in Transverse Direction.

3.3 Comparison of Spanwise Structures

In order to visualize the evolving structures from the instantaneous velocity field of nozzle and orifice jets a filtering scheme was adopted. The 2D velocity field contains flow structures of different scales, which are not directly visible from the instantaneous velocity field obtained by PIV. The smaller scales may not be captured by PIV due to inadequate spatial resolution as mentioned earlier. The application of spatial filtering has been shown to be more effective in bringing out the structures compared to the conventional Reynolds averaged filtering (Piirto et al., 2001). This spatial filtering scheme is equivalent to FFT filtering in frequency domain. The spatial filter kernel in this work uses the same as used by Reuss et al. (1990).

The Gaussian kernel with weighting function

$$w(k,m) = e^{(-2(k^2+m^2)/p^2)} \tag{5}$$

(where k and m are spatial mask sizes and p the grid spacing constant.)

p determines the degree to which the algorithm smoothes the u and v velocity matrices. A number of variations of this method can be used: different kernels, (like swirl, gradient, etc.) a large or smaller grid spacing constant *(p);* and a large or smaller mask size (the extent of k and m*).* The value of p is a factor which represents the width across which the kernel smoothes within a cell. Reuss (1990) suggests that p should be set in accordance with the grid spacing of the interrogation cell such that kernel goes to zero near edge or the boundary of the mask. The kernel size k and m for the present studies in terms of interrogation cells are varied to 6, 16 and 24 that provided a spatial area of 18 x 18 mm, 48 x 48 mm and 72 x72 mm respectively. At the edge of this mask, k/p value was 0.07.

The instantaneous velocity field is convolved with the above Gaussian kernel to obtain local averaged velocity field U^s_{ij} and V^s_{ij} by using the relation given below

$$U^s_{ij} = \frac{\sum_{-m}^{m}\sum_{-k}^{k}\left[w(k,m)U_{i-k,j-m}\right]}{W} \tag{6}$$

$$V^s_{ij} = \frac{\sum_{-m}^{m}\sum_{-k}^{k}\left[w(k,m)V_{i-k,j-m}\right]}{W} \tag{7}$$

The denominator

$$W = \sum_{-m}^{m}\sum_{-k}^{k} w(k,m) \tag{8}$$

can be considered as weighted area of Gaussian kernel for normalization. The instantaneous velocity difference field for any typical PIV frame of velocity field is defined as

$$\hat{u}_{i,j} = u_{i,j} - U^s_{i,j} \quad \text{and} \quad \hat{v}_{i,j} = v_{i,j} - V^s_{i,j} \tag{9}$$

Vorticity from the $\hat{u}_{i,j}$ and $\hat{v}_{i,j}$ was computed using a simple forward difference scheme. Figure 8 shows the vorticity field for nozzle (minor axis) for a kernel size of 48 mm. Here the presence of large-scale structures in the shear layer is clearly visible. The high intensity positive and negative (red and blue) vorticity regions properly identify the counter clockwise and clockwise vortex structures. The intensity and coherence of eddies are seen to decrease with downstream positions. From the nature of the structures seen from the different frames of 2D PIV data in the major and minor axis planes it is observed that the average extent of the vortical structures and inter vortical spacing remain nearly the same for both major and minor planes. The characteristic scale of separation ranges from 20 to 40 mm, depending on the strength and shape of the individual structures. The size of the structure is estimated to be 20 to 30 mm.

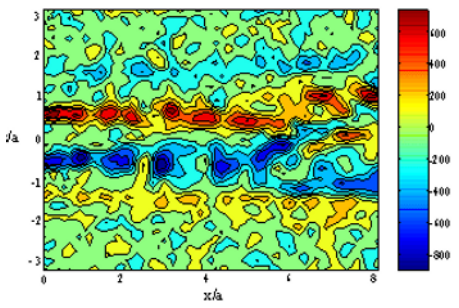

Fig. 8. Vorticity Field from the Spatially Filtered Velocity Data in Nozzle Jet.

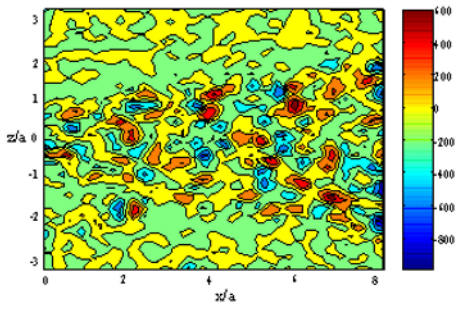

Fig. 9. Vorticity Field from the Spatially Filtered Velocity Data in Orifice Jet.

The spatial filtering already described was similarly applied to the orifice flow data. With spatial filtering kernels of sizes 6, 18 and 24 it was not possible to identify any organized structures. The iso-vorticity contours of spatially filtered field in the minor plane for the kernel size of 16 (48 x 48 mm) is shown in Fig. 9. In contrast to that of the nozzle there does not seem to be one dominant vortex ring at the exit in the vorticity field. The frame shows that both positive and negative vorticity regions adjacent to one another all over the field suggesting smaller vortex rings are very active. It is very difficult to see the unique connectivity of these rings except close to the jet exit. Near the exit plane of the orifice it may be possible to identify two small vortex rings on the edges of the shear layer. Further downstream these vortex rings seem to be distributed over the entire field, oriented possibly in different directions.

The main features that differentiate the development of a nozzle jet and orifice jet are the following. a.) While turbulence intensities are higher in orifice jet, associated turbulence length scales are smaller and do not grow, when compared to nozzle jet. b.) While large scale structures are seen in the nozzle jet they are totally absent in the orifice jet. Instead dominant smaller scale vortex rings which are likely to be in the energy containing scale are seen. The smaller dominant vortex rings could be attributed to very sharp shear layer with zero momentum and thickness in the orifice jet. These intense energy containing scale leads to higher turbulence intensity in the orifice jet. Studies of Ramesh (2003) show that in the orifice jet the peak intensity of turbulence in the minor plane is larger than the peak intensity in the major plane. Also when the vortex rings are convected by the mean field their orientation changes and they generate axial vortex field. The interaction of the small scale azimuthal vortices with axial vortex field could be reason for the enhanced growth in the minor plane and the reduction in the axis switching distance of orifice jet.

4. Conclusion

The PIV measurements were carried out to document the spatial characteristics of 2:1 aspect ratio elliptic jets issuing from a contoured nozzle and sharp edged orifice at a Reynolds number of 72000. The two point spatial correlation in the shear layers reveals the streamwise and spanwise distribution of the integral scales based on the streamwise fluctuations. The shapes of these correlation functions were found to be different between nozzle and orifice jets. The visualization of the vortical structures using the novel spatial filtering scheme also support the results of the two point correlation by indicating a single vortex ring in the case of nozzle and breakdown to smaller vortical structures in the case of orifice. Earlier studies mostly on nozzles attributed axis switching to the self-induction process. However the axis switching mechanism could be different in the case of orifice where the small-scale highly intense vortex rings are convected and distorted creating further streamwise vortices. These streamwise vortices and also the basic average azimuthal vortex field may be the cause of intense mixing and could result in large reduction of axis switching distance.

References

Brown, G. and Roshko, A., On density effects and large structure in turbulent mixing layers, Journal of Fluid Mechanics, 64 (1974), 775-816.

Crow, S. C. and Champange, F. H., Orderly structure in jet turbulence, Journal of Fluid Mechanics, 48 (1971), 547.

Davis, D. O. and Gessner, Experimental investigation of turbulent flow through a circular-to-rectangular transition duct, AIAA Journal, 30 (1992), 367- 375.

Eriksson, J. G. and Karlsson, R. I., An investigation of the spatial resolution requirements for two point correlation measurements using LDV, Experiments in Fluids, 18 (1998), 393-396.

Hinze, J. O., Turbulence, (1975), 39-58, McGraw-Hill.

Ho, C. M. and Gutmark, E., Vortex Induction and mass entrainment in a small-aspect-ratio jet, Journal of Fluid Mechanics, 179 (1987), 383-405.

Hussain, F. and Husain, H. S., Elliptic jets, Part 1: Characteristic of unexcited and excited jets, Journal of Fluid Mechanics, 208 (1989), 257-320.

Krothapalli, A., Baganoff, D. and Karamcheti, K., On the Mixing of a Rectangular Jet, Journal of Fluid Mechanics, 107 (1981), 201-220.

Oakley, T., Loth, E. and Adrian, R. J., Cinematic PIV of high-Reynolds-number turbulent free shear layer, AIAA Journal, 34 (1995), 299-308.

Paschal, K., Yao, C. and Ulrich, S., Spatial resolution effects on PIV measurements in turbulent wake flow, Fluid Dynamics Conference, 28th (Colorado Springs), (1994), 2294-2297.

Piirto, M., Ghalainen, H., Elonanta, H. and Saarenrinne, P., 2D spectral and turbulence length scale estimation with PIV, Journal of Visualization, 4-1 (2001).

Quinn, W. R., On mixing in an elliptic turbulent free Jet, Physics of Fluids, 1-10 (1989), 1716-1722.

Ramesh, G., Venkatakrishnan, L. and Madhavan, K. T., PIV studies in small aspect ratio elliptic jet: Effect of spatial resolution, DVR on turbulence, Proc. of the 7th Intl. Symposium on Flow Measurements and control, (Sorrento, Italy), (2003-8).

Ramesh, G., PIV Studies in Small Aspect Ratio Elliptic Jets, (2003-8), PhD Thesis, Indian Institute of Science.

Reuss, L. R., Bardsley, M., Felton, P. G., Landreth, C. C. and Adrian, R. J., Velocity, Vorticity, and Strain-rate ahead of a flame measured in an engine using Particle Image Velocimetry, SAE Technical paper, (1990), 1-17.

Sang, Lee J. and Beak, S. J., The Effect of Aspect Ratio on the Near Field Structure of Elliptic Jets, Journal of Flow Measurements and Instrumentation, 5-2 (1990), 170-180.

Zaman, K. B. MQ., Axis switching and spreading of an asymmetric jet: The role of coherent structure dynamics, Journal of Fluid Mechanics, 316 (1996), 1-27.

Author Profile

Ramesh, G.: He received his M.Sc. (Eng) in Instrumentation engineering in 1998 and Ph.D. in Instrumentation engineering in 2004 from Indian Institute of Science, Bangalore. He works in the Experimental Aerodynamics Division of National Aerospace laboratories, Bangalore, India. His areas of interest are Quantitative visualization, LDV and Wind tunnel instrumentation,

Venkatakrishnan, L.: He received his M.Tech in 1991 in Aerospace engineering from Indian Institute of Technology Bombay and his Ph.D. in 1997 from Indian Institute of Science, Bangalore. He works in the Experimental Aerodynamics Division of National Aerospace laboratories, Bangalore, India. His research interests are flow diagnostics and aeroacoustics.

Prabhu, A.: He received his M.Tech. in Aeronautical engineering in 1963 from Indian Institute of Science (IISc) and PhD in Aerospace in 1971 from the same institute. He is presently working as an emeritus professor in Aerospace Department after his retirement from service as professor at IISc. His research interests are turbulence in lab scales as well as in the atmosphere.